Detection of Double Resonance by Frequency Change: Application to Hg^{201}†

ROBERT H. KOHLER*
Department of Physics and Research Laboratory of Electronics, Massachusetts Institute of Technology, Cambridge, Massachusetts
(Received September 27, 1960)

A new type of double-resonance experiment that depends on wavelength effects rather than on polarization effects is discussed. Incident polarized light is replaced by incident light of wavelength coincident with just one component of the structure to be measured. The analyzer is replaced by a cell of gas that absorbs just that same component and lets the others pass. Magnetic resonance from the excited component to one of the others is monitored by increases in the light transmitted through the absorbing gas. This experiment requires that the Doppler width be smaller than the structure. This method was first applied to measure the hyperfine structure of the $^3P_1$ state of Hg^{201}. The incident light and absorbing gas were both supplied by separated Hg^{198}, whose resonance line coincides naturally with one component of the Hg^{201} hyperfine structure. Measurement of Hg^{201} is discussed in detail. The following hfs intervals were found: $f(\frac{1}{2}\leftrightarrow\frac{3}{2})=7551.613\pm0.013$ Mc/sec and $f(\frac{3}{2}\leftrightarrow\frac{5}{2})=13\,986.557\pm0.008$ Mc/sec. The magnetic dipole and electric dipole interaction constants, calculated without quadratic hfs corrections, are $a=-5454.569\pm0.003$ Mc/sec, $b=-280.107\pm0.005$ Mc/sec.

Means for applying the method when there is no isotope coincidence are given. This new method is compared with the polarization technique and is found to give signal-to-noise ratios that are orders of magnitude higher.

I. NEW DOUBLE-RESONANCE METHOD APPLIED TO Hg^{201}

THE new type of experiment discussed here was first performed[1,2] on the hyperfine structure of Hg^{201}, $^3P_1$. Special features of the 2537 A resonance line were employed. Hg^{201} has three components that are separated by intervals that are much larger than their optical Doppler widths. Hg^{198} has a single component that coincides with the center Hg^{201} component. (See Figs. 1 and 2.)

The apparatus is shown in Fig. 3. Light from an Hg^{198} lamp excites just the $F=\frac{3}{2}$ component of Hg^{201} atoms in the resonance cell. Light reradiated from these atoms passes into an absorption cell containing Hg^{198} vapor. In the absence of any microwave transitions, the wavelength of this reradiated light is essentially that of the Hg^{198} resonance line. This light is, accordingly, scattered by the Hg^{198} atoms in the absorption cell and only a fraction of it gets through to the photomultiplier.

When the microwave field is at the resonant frequency, for transitions to either $F=\frac{1}{2}$ or $F=\frac{3}{2}$, the wavelength of such reradiated light is no longer at the Hg^{198} resonance line and the light suffers no attenuation in the absorption cell.

Thus the microwave resonance is detected as an increase in the output of the photomultiplier.[2a]

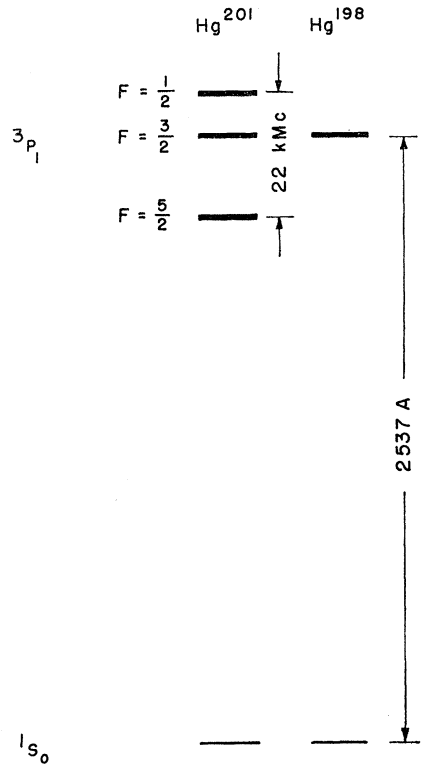

FIG. 1. Resonance lines of Hg^{201} and Hg^{198}.

† This work, which is based on a Ph.D. thesis, Department of Physics, Massachusetts Institute of Technology, August, 1960, was supported in part by the U. S. Army (Signal Corps), the U. S. Air Force (Office of Scientific Research, Air Research and Development Command), and the U. S. Navy (Office of Naval Research).

* Present address, Columbia Radiation Laboratory, Physics Department, Columbia University, New York.

[1] R. H. Kohler, Quarterly Progress Report, Research Laboratory of Electonics, Massachusetts Institute of Technology, July 15, 1956 (unpublished), pp. 20–21.

[2] R. H. Kohler, Quarterly Progress Report, Research Laboratory of Electronics, Massachusetts Institute of Technology, January 15, 1958 (unpublished), p. 39.

[2a] Bucka has performed a double resonance experiment with a geometry similar to that described here, but with a somewhat different principle of operation. The lamp, resonance cell, and absorption cell each contain the same isotope, one whose resonance line shows resolved hyperfine structure. There is slightly selective excitation in the resonance cell, and slightly selective absorption in the absorption cell. See Z. Physik **151**, 328 (1958).

A. Zeeman Effect of the Hyperfine Structure

For ease in scanning through the microwave resonance, a weak dc magnetic field is applied, and each microwave resonance is split into several resonances by a calculable Zeeman effect (Fig. 4) in the region that is linear with small quadratic corrections.

The value for the linear energy change[3,4] is $g_F\mu_B H_{dc}M$, and

$$g_F=g_J\frac{F(F+1)+J(J+1)-I(I+1)}{2F(F+1)}-g_I\frac{F(F+1)+I(I+1)-J(J+1)}{2F(F+1)};$$

$g_J=\frac{3}{2}$ (based on L, S coupling);

$g_J=1.4838\pm0.0004$ (measured[3]).

See Table I.

The quadratic energy-level change, from second-order perturbation theory, is given by

$$g_J^2\mu_B^2H_{dc}^2\cdot\sum_{F\neq F'}\frac{|\langle FM|J_z|F'M\rangle|^2}{E_F-E_{F'}}.$$

These changes are tabulated in Table II.

The shifts in transition frequencies with magnetic field are calculated by subtracting the corresponding energy levels. (Tables III and IV and Figs. 5 and 6.)

TABLE I. Calculation of values of g_F for Hg^{201}, $^3P_1$.

F	g_F (approx)	g_F (exact)	$gF(\mu B/h)$ [(Mc/sec)/gauss]
$\frac{5}{2}$	$\frac{3}{5}$	$\frac{2}{5}g_J+1.19\times10^{-4}$ $=0.59352\pm0.0002$	0.83074 ± 0.0004
$\frac{3}{2}$	$\frac{2}{5}$	$(4/15)g_J+1.46\times10^{-4}$ $=0.39573\pm0.0001$	0.55390 ± 0.0002
$\frac{1}{2}$	-1	$-\frac{2}{3}g_J+3.31\times10^{-4}$ $=-0.98887\pm0.0003$	-1.38411 ± 0.0007
		$g_J=1.4838\pm0.0004$	
		$\mu_I=-0.55153$ nm	

B. Line Shape of the Resonances

The line shape is determined by the microwave transition probability, $w(t)$, between two given levels in the ^3P state and by the probability, $e^{-t/\tau}/\tau$, that the atom has not left this state (the lifetime, τ, is approximately 10^{-8} sec). The total probability,[3] $\bar{P}$, that one atom will have made a microwave transition is $\int_0^\infty(e^{-t/\tau}/\tau)w(t)dt$.

[3] J. Brossel and F. Bitter, Phys. Rev. **86**, 308 (1952).
[4] E. U. Condon and G. Shortley, *The Theory of Atomic Spectra* (Cambridge University Press, New York, 1953).

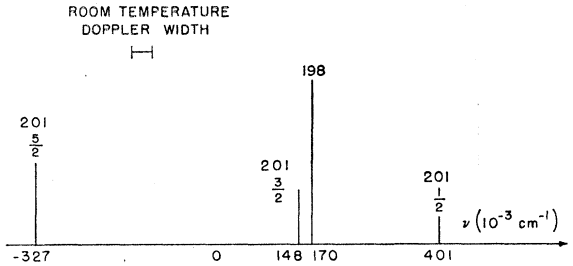

FIG. 2. Hyperfine structure of the 2537 A line of Hg^{201} and Hg^{198} (from data of Young[19]).

If the applied microwave frequency is close to only one possible resonance,[5] then

$$w(t)=\frac{a_{rs}^2\sin^2\{\frac{1}{2}t[(\omega-\omega_{rs})^2+a_{rs}^2]^{\frac{1}{2}}\}}{(\omega-\omega_{rs})^2+a_{rs}^2},$$

where

$$a_{rs}^2=(g_J\mu_B/\hbar)^2|\langle FM|\mathbf{H}_{rf}\cdot\mathbf{J}|F'M'\rangle|^2,$$

$\omega_{rs}/2\pi=f_{rs}$=frequency difference between the two states, $\omega/2\pi=f$=frequency of applied microwave field. Performing the indicated integration yields

$$\bar{P}=\tfrac{1}{2}a_{rs}^2\Big/\left[(\omega-\omega_{rs})^2+a_{rs}^2+\frac{1}{\tau^2}\right].$$

This expression is Lorentzian with a frequency half-width of $(\pi\tau)^{-1}$ for small a_{zs}^2. $\bar{P}$ gives the line shape. In practice, ω is held fixed, and ω_{rs} is varied linearly with the magnetic field according to Figs. 5 and 6 or Tables III and IV to give a Lorentzian in magnetic field.

C. Microwave Transition Probabilities

The strength of the resonance at the center of the line, for weak rf fields, is

$$\tfrac{1}{2}g_J^2\mu_B^2(\tau^2/\hbar^2)|\langle FM|\mathbf{H}_{rf}\cdot\mathbf{J}|F'M'\rangle|^2=\bar{P}_c.$$

The nonzero matrix elements, calculated from the following expressions,[4] are given in Tables V and VI:

$$|\langle FM|J_z|F-1M\rangle|^2=A^2(F+M)(F-M),$$
$$|\langle FM|J_x|F-1M+1\rangle|^2=\tfrac{1}{4}A^2(F-M)(F-M-1),$$
$$|\langle FM|J_x|F-1M-1\rangle|^2=\tfrac{1}{4}A^2(F+M)(F+M-1),$$
$$A=\frac{(F-J+I)(F+J+I)(J+I+1+F)(J+I+1-F)}{4F^2(2F-1)(2F+1)}.$$

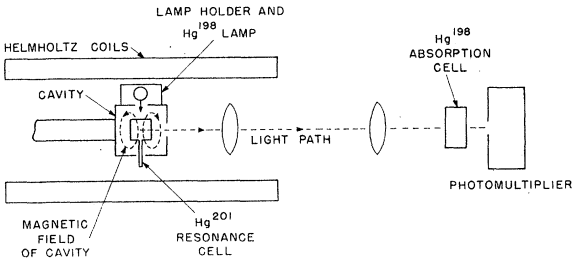

FIG. 3. Diagram of apparatus.

[5] N. H. Ramsey, *Molecular Beams* (Clarendon Press, Oxford, 1956).

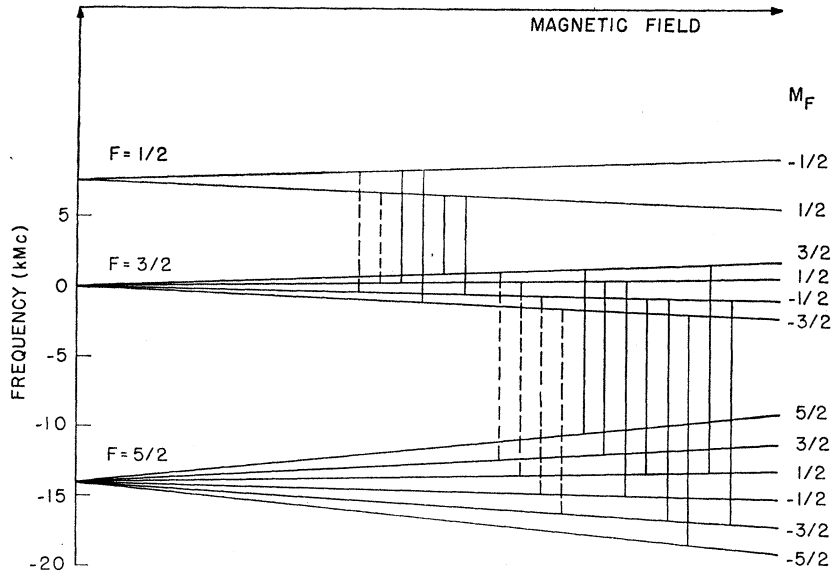

FIG. 4. Zeeman effect of the hyperfine structure of Hg^{201}, $^3P_1$ showing possible transitions.

D. Signal Strengths

Signal strengths may be computed conveniently for two limiting cases. In the first case the incident light strikes the face of the resonance cell from a large solid angle, and there is multiple scattering in the cell before and after the microwave transition. Each atom receives light from all directions uniformly or has all of the Zeeman substates of $F=\frac{3}{2}$ state equally populated. Multiple scattering after the transition insures that any directional preferences in the reradiated light are lost. The amplitudes of the resonances are proportional to the transition probabilities. The relative change in observed light is $\bar{P}_c(1-\phi)/4\phi$, where $\bar{P}_c$ refers to the resonance in question, and ϕ is the transmission of the absorption cell for light reradiated from the $F=\frac{3}{2}$ state (see Appendix).

In the second case the incident light is strictly parallel to the direction of the magnetic field and is scattered only once before leaving the resonance cell. Here angular distribution effects may be computed from Fig. 7. The vertical lines represent π transitions, the oblique, σ transitions.[4] Both refer to either absorption or spontaneous emission.

Light that is incident and parallel to the magnetic

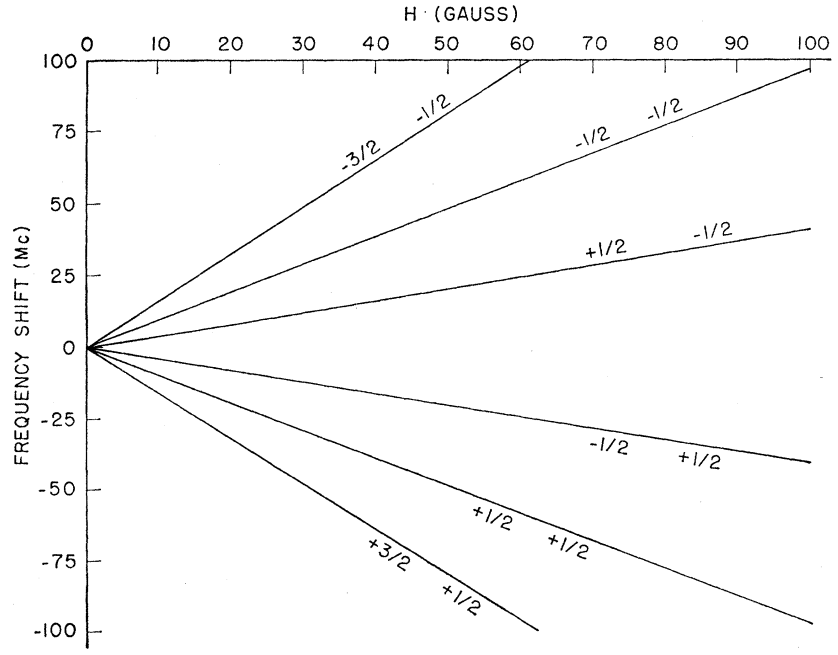

FIG. 5. Frequency shift as a function of magnetic field for $F=\frac{3}{2} \rightarrow F=\frac{1}{2}$ interval.

TABLE II. Quadratic energy level changes in magnetic field.

F	M	$(E_{FM}^{(2)}-E_F)/g_J^2\mu_B^2H^2$	$(E_{FM}^{(2)}-E_F)/h^2H^2$[(Mc/sec)/gauss^2]
$\frac{5}{2}$	$\pm\frac{5}{2}$	0	0.000
$\frac{5}{2}$	$\pm\frac{3}{2}$	$\lvert\langle\frac{5}{2}\pm\frac{3}{2}\rvert J_z\rvert\frac{3}{2}\pm\frac{3}{2}\rangle\rvert^2/(E_{5/2}-E_{3/2})$	-0.744×10^{-4}
$\frac{5}{2}$	$\pm\frac{1}{2}$	$\lvert\langle\frac{5}{2}\pm\frac{1}{2}\rvert J_z\rvert\frac{3}{2}\pm\frac{1}{2}\rangle\rvert^2/(E_{5/2}-E_{3/2})$	-1.12×10^{-4}
$\frac{3}{2}$	$\pm\frac{3}{2}$	$\lvert\langle\frac{3}{2}\pm\frac{3}{2}\rvert J_z\rvert\frac{5}{2}\pm\frac{3}{2}\rangle\rvert^2/(E_{3/2}-E_{5/2})$	$+0.744\times10^{-4}$
$\frac{3}{2}$	$\pm\frac{1}{2}$	$\lvert\langle\frac{3}{2}\pm\frac{1}{2}\rvert J_z\rvert\frac{1}{2}\pm\frac{1}{2}\rangle\rvert^2/(E_{3/2}-E_{1/2})$ $+\lvert\langle\frac{3}{2}\pm\frac{5}{2}\rvert J_z\rvert\frac{5}{2}\pm\frac{1}{2}\rangle\rvert^2/(E_{3/2}-E_{5/2})$	$-3.17\times10^{-4}+1.12\times10^{-4}$ $=-2.05\times10^{-4}$
$\frac{1}{2}$	$\pm\frac{1}{2}$	$\lvert\langle\frac{1}{2}\pm\frac{1}{2}\rvert J_z\rvert\frac{3}{2}\pm\frac{1}{2}\rangle\rvert^2/(E_{1/2}-E_{5/2})$	$+3.17\times10^{-4}$

field is composed one half of σ^+, and one half of σ^-. The resulting relative occupation numbers for the $F=\frac{3}{2}M$ sublevels $(-\frac{3}{2}, -\frac{1}{2}, \frac{1}{2}, \frac{3}{2})$ are (3,7,7,3), respectively.

We define the following symbols: n_r=occupation number of a given state; π_r=number of π radiations from a state with occupation number of 1; σ_r^+=number of σ^+ radiations from a state with occupation number of 1; $\sigma=\sigma^++\sigma^-$; I_1=intensity of light observed in x direction, no resonance; I_2=intensity in x direction, with resonance; $\rho=(I_2-I_1)/I_1$=signal strength; $K=30=\sigma+\pi$ for any M sublevel in $^3P_1$.

The intensity observed in the x direction is twice as great for a π transition as for a σ^+ or σ^- transition. Then, for transitions from $r=(\frac{3}{2},M')$ to $s=(F,M'')$, we have

$$I_1=\phi\sum_M n_{\frac{3}{2},M}(2\pi_{\frac{3}{2},M}+\sigma_{\frac{3}{2},M}),$$

$$I_2=I_1-\bar{P}_c\phi n_{\frac{3}{2},M'}(2\pi_{\frac{3}{2},M'}+\sigma_{\frac{3}{2}M'})+\bar{P}_c n_{\frac{3}{2},M'}(2\pi_{FM'}+\sigma_{FM'}),$$

$$\rho=\frac{\bar{P}_c n_{\frac{3}{2}M'}[(1-\phi)K+\pi_{FM''}-\phi\pi_{\frac{3}{2}M'}]}{\phi(K\sum_M n_{\frac{3}{2}M}+\sum_M n_{\frac{3}{2}M}\pi_{\frac{3}{2}M})}.$$

For $\phi=1$ (no absorption cell),

$$\rho=\bar{P}_c n_{\frac{3}{2}M'}\frac{(\pi_{FM''}-\pi_{\frac{3}{2}M'})}{(K\sum_M n_{\frac{3}{2}M}+\sum_M n_{\frac{3}{2}M}\pi_{\frac{3}{2}M})}.$$

For $\phi\ll1$ (a very good absorption cell),

$$\rho=\frac{\bar{P}_c n_{\frac{3}{2}M'}(K+\pi_{FM'})}{\phi(K\sum_M n_{\frac{3}{2}M}+\sum_M n_{\frac{3}{2}M}\pi_{\frac{3}{2}M})}.$$

For the transitions used in the experiment, case 2 (Table VII) agrees with case 1 within a factor of 2 in the limit of small ϕ.

II. APPARATUS FOR THE Hg^{201} EXPERIMENT

This apparatus is shown in Fig. 3. The microwave power is off-on modulated at 30 cps so that the light increase at resonance will be modulated so as to be more easily extracted from the background. This extraction is accomplished by using an ac narrow-band amplifier peaked at 30 cps following the photomultiplier.

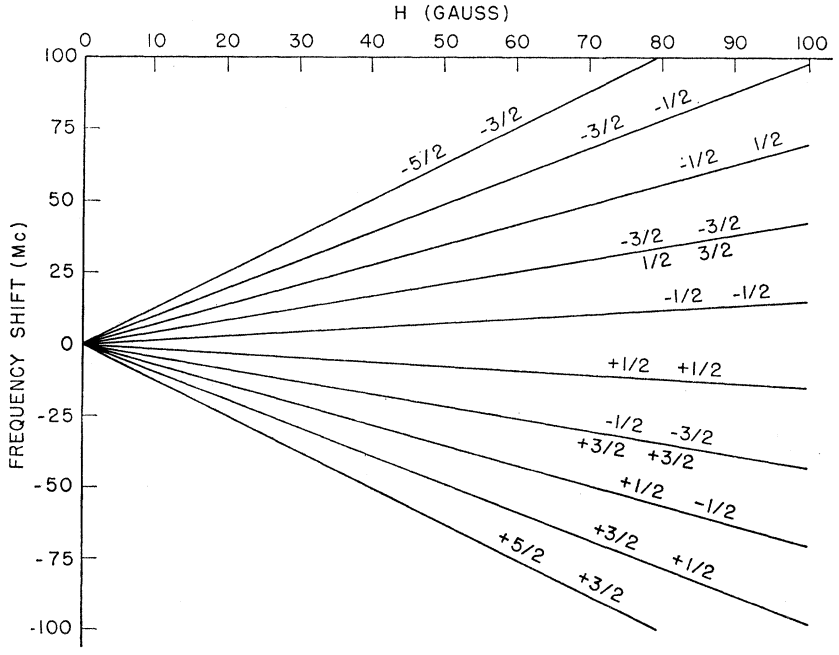

FIG. 6. Frequency shift as a function of magnetic field for the $F=\frac{5}{2}\rightarrow F=\frac{3}{2}$ interval.

TABLE III. Frequency shift as a function of magnetic field for the $F=\frac{3}{2}\rightarrow F=\frac{1}{2}$ interval.

$M_{3/2}$	$M_{1/2}$	$h\Delta f/\mu_B H$	Approximate $\Delta f/H$ (Mc/sec)/gauss	Exact Frequency shift (Mc/sec) (H in gauss)
$-\frac{1}{2}$	$-\frac{1}{2}$	+7/10	+0.979	$+0.96900H+0.000522H^2$
$+\frac{1}{2}$	$+\frac{1}{2}$	−7/10	−0.979	$-0.96900H+0.000522H^2$
$-\frac{3}{2}$	$-\frac{1}{2}$	+11/10	+1.54	$+1.52290H+0.0002426H^2$
$+\frac{3}{2}$	$+\frac{1}{2}$	−11/10	−1.54	$-1.52290H+0.0002426H^2$
$-\frac{1}{2}$	$+\frac{1}{2}$	−3/10	−0.420	$-0.41510H+0.000522H^2$
$+\frac{1}{2}$	$-\frac{1}{2}$	+3/10	+0.420	$+0.41510H+0.000522H^2$

The background, which arises from the light that gets through the absorption cell in the absence of microwave transitions, carries noise[6] with it. The noise-to-dc background ratio is $(2e\Delta f/i_K)^{\frac{1}{2}}=(2\Delta f/n_\rho)^{\frac{1}{2}}$, where i_K is the dc photocathode current, e is the electronic charge, Δf is the bandwidth of the amplifier, and n_ρ is the product of the light flux at the photocathode and the photocathode efficiency.

If the noise-to-dc background ratio with the cell removed is α, and the signal strength is $\bar{P}/4\alpha$ (case 1), then the noise-to-dc background ratio with the cell in place is $\alpha/\sqrt{\phi}$, and the signal-to-noise ratio is $\bar{P}/4\alpha\sqrt{\phi}$. The measured value of α was approximately 3×10^{-4} for an amplifier bandwidth of 0.2 cps.

A. Optics

The lamp was of the electrodeless discharge type. The Hg^{198} sample is contained in a sealed-off section of 5-mm o.d. quartz tubing. The tubing is placed at the end of a coaxial microwave line in the place normally occupied by the center conductor. The line was powered with a 10-cm cw magnetron (QK61) fed by a regulated power supply. The lamp was cooled laterally by a flow-regulated and ice-bath-cooled dry nitrogen blast. The lamp was operated with partial self-reversal.

For each of the two ΔF transitions, the resonance cell was an evacuated quartz chamber, charged with 60% enriched Hg^{201}, and sealed off. The cell for the 7.6-kMc/sec transition is basically a section of 12-mm o.d. tubing with a flat window fused onto one end. The cell for the 14-kMc/sec transition is shown in Fig. 8. The small size of the cell necessitated the use of special care in producing a flat window at the left end. A flat quartz disk and the 7-mm section were each ground to perfectly matching 45° bevels. Fusion was then possible with a relatively cool flame, which did not distort the window. Both cells were operated at room temperature, at which approximately half of the incident radiation is intercepted and multiple scattering is present.

TABLE IV. Frequency shift as a function of magnetic field for the $F=\frac{5}{2}\rightarrow F=\frac{3}{2}$ interval.

$M_{5/2}$	$M_{1/2}$	$h\Delta f/\mu_B H$	Approximate $\Delta f/H$ (Mc/sec)/gauss	Exact Frequency shift (Mc/sec) (H in gauss)
$-\frac{3}{2}$	$-\frac{3}{2}$	+3/10	+0.420	$+0.41526H+0.0001488H^2$
$+\frac{3}{2}$	$+\frac{3}{2}$	−3/10	−0.420	$-0.41526H+0.0001488H^2$
$-\frac{1}{2}$	$-\frac{1}{2}$	+1/10	+0.140	$+0.13842H-0.000093H^2$
$+\frac{1}{2}$	$+\frac{1}{2}$	−1/10	−0.140	$-0.13842H-0.000093H^2$
$-\frac{5}{2}$	$-\frac{3}{2}$	+9/10	+1.26	$+1.24600H+0.0000744H^2$
$+\frac{5}{2}$	$+\frac{3}{2}$	−9/10	−1.26	$-1.24600H+0.0000744H^2$
$-\frac{3}{2}$	$-\frac{1}{2}$	+7/10	+0.979	$+0.96916H-0.0001306H^2$
$+\frac{3}{2}$	$+\frac{1}{2}$	−7/10	−0.979	$-0.96916H-0.0001306H^2$
$-\frac{1}{2}$	$+\frac{1}{2}$	+5/10	+0.700	$+0.69232H-0.000093H^2$
$+\frac{1}{2}$	$-\frac{1}{2}$	−5/10	−0.700	$-0.69232H-0.000093H^2$
$-\frac{1}{2}$	$-\frac{3}{2}$	−3/10	−0.420	$-0.41548H+0.0001864H^2$
$+\frac{1}{2}$	$+\frac{3}{2}$	+3/10	+0.420	$+0.41548H+0.0001864H^2$

[6] R. Engstrom, J. Opt. Soc. Am. **37**, 420 (1947).

TABLE V. Nonzero matrix elements for $\Delta M=0$.

F	F'	M	$\lvert\langle FM\lvert J_z\rvert F'M\rangle\rvert^2$
$\frac{1}{2}$	$\frac{3}{2}$	$\pm\frac{1}{2}$	10/18
$\frac{3}{2}$	$\frac{5}{2}$	$\pm\frac{3}{2}$	24/100
		$\pm\frac{1}{2}$	36/100

The Hg^{198} absorption cell provided a 1-cm absorption path and was operated at room temperature. The only impurity in this Hg^{198} was 0.22% of Hg^{201}.

The measured value of ϕ was approximately 0.20. The calculated value (see Appendix) with the assumption of a very broadband exciting line and single scattering out of the resonance cell was 0.18. The calculated value with the assumption of a Doppler exciting line and single scattering out of the resonance cell was 0.01. Approximately one-third of the output of the photomultiplier was from stray lamp light that is outside of the 2537 A Hg^{198} line.

Schemes to obtain a better value for ϕ would require elimination of this stray light in order to be effective. These schemes were not undertaken because of the high signal-to-noise ratio already available.

B. Microwave System

Two distinct sets of microwave equipment were required, one for each of the two ΔF resonances. The schematic diagram shown in Fig. 9 is suitable for either one.

Each cavity operated in a TE mode[7] of a right

TABLE VI. Nonzero matrix elements for $\Delta M=\pm1$.

F	F'	M	M'	$\lvert\langle FM\lvert J_x\rvert F'M'\rangle\rvert^2$
$\frac{1}{2}$	$\frac{3}{2}$	$\pm\frac{1}{2}$	$\pm\frac{3}{2}$	15/36
		$\pm\frac{1}{2}$	$\mp\frac{1}{2}$	5/36
$\frac{3}{2}$	$\frac{5}{2}$	$\pm\frac{3}{2}$	$\pm\frac{5}{2}$	30/100
		$\pm\frac{1}{2}$	$\pm\frac{3}{2}$	18/100
		$\pm\frac{1}{2}$	$\mp\frac{1}{2}$	9/100
		$\pm\frac{3}{2}$	$\pm\frac{1}{2}$	3/100

[7] C. G. Montgomery, *Technique of Microwave Measurements*, Radiation Laboratory Series (McGraw-Hill Book Company, Inc., New York, 1947), Vol. 11.

TABLE VII. Calculated relative change in intensity (case 2).

Transition	$F=\frac{3}{2}, M=\pm\frac{1}{2}$ to $F=\frac{1}{2}, M=\pm\frac{1}{2}$	$F=\frac{3}{2}, M=\pm\frac{1}{2}$ to $F=\frac{5}{2}, M=\pm\frac{1}{2}$	$F=\frac{3}{2}, M=\pm\frac{3}{2}$ to $F=\frac{5}{2}, M=\pm\frac{3}{2}$
General	$\bar{P}_c(7)(40-32\phi)/\phi(736)$	$\bar{P}_c(7)(48-32\phi)/\phi(736)$	$\bar{P}_c(3)(42-48\phi)/\phi(736)$
No absorption cell	$\bar{P}_c(7)(8)/736=(0.0761)\bar{P}_c$	$\bar{P}_c(7)(16)/736=(0.152)\bar{P}_c$	$\bar{P}_c(3)(-6)/736=-(0.0244)\bar{P}_c$
Good absorption cell	$\bar{P}_c(7)(40)/\phi(736)=\bar{P}_c(0.380)/\phi$	$\bar{P}_c(7)(48)/\phi(736)=\bar{P}_c(0.456)/\phi$	$\bar{P}_c(3)(42)/\phi(736)=\bar{P}_c(0.171)/\phi$

circular cylinder with one end wall on a movable plunger for tuning. The 7.6-kMc/sec cavity operated in the TE_{021} mode. The optical exit aperture was covered with gauze to prevent lowering of the cavity Q by radiative losses. The resonance cell had almost no effect on the Q. The 14-kMc/sec cavity operated in the TE_{011} mode. This cavity did not present the troublesome double moding that the other cavity did. The optical exit aperture consisted of 0.012-inch slits normal to the axis of the cylinder. These had no affect on the cavity Q. The resonance cell lowered the Q only 25%. Larger cells lowered it drastically.

The interrupter is a mechanical device for providing 30-cps full modulation of the microwave power. The device consists of a semicircular blade of carbonized resistance board mounted on the shaft of a 30-cps synchronous motor and passing into a section of waveguide through a paraxial slit on the face of the waveguide.

The sampling section picks up a small sample of the line power for frequency monitoring. In a crystal multiplier-mixer this sample is beaten with a harmonic of the frequency standard at approximately 950 Mc/sec the frequency difference being kept close to zero. The frequency standard is accurate to one part in 10^7. It consists of a combination of a Gertsch FM4A chasis, a Gertsch FM6 chassis, and a Hewlett-Pack and frequency counter.

The klystrons were connected with the shells grounded. The cathode-to-reflector voltage was supplied by a battery pack, with a provision for continuous adjustment over a small range. For the 7.6-kMc/sec and 14-kMc/sec systems a Sperry 2K39 and Varian VA92C were used. Short-term drifts of 70 kc/sec and 35 kc/sec were encountered. Long-term drifts were eliminated by manual adjustments of the reflector voltage.

The calculated fields at the center of the cavity for full power were approximately 0.3 gauss and 1.0 gauss for the 7.6-kMc/sec and 14-kMc/sec systems, respectively.

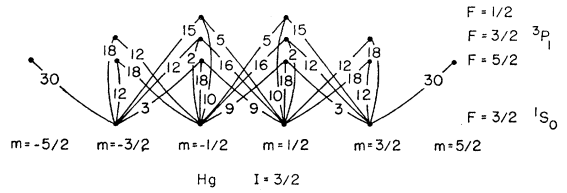

FIG. 7. Optical transition probabilities for the components of the resonance line of Hg^{201}.

C. DC Magnetic Field

The steady field was supplied by Helmholtz coils that were powered by submarine batteries and controlled manually by variable resistors. The coils could produce a maximum field of 75 gauss. The current was monitored with a potentiometer and an ice-cooled shunt. An absolute calibration was made by means of proton resonance, but this was not essential for determining the zero-field frequencies because linear extrapolation was used.

D. Detection System

The detection system consisted of a 1P28 photomultiplier followed by a 30-cps ac narrow-band phase-sensitive amplifier of 0.2-cps bandwidth.

III. RESULTS FOR THE Hg^{201} EXPERIMENT

Locations of the resonances and approximate values of the ΔF frequencies were determined by manual adjustments of the frequency of the microwave field in zero dc field. Here all of the Zeeman resonances overlap and thus give high signal strength. Precise measurements were made by reducing the microwave power to eliminate power broadening; then the signal-to-noise ratio was a few hundreds. The microwave frequency was kept fixed at various values, and the dc field was swept manually over resonance.

For every frequency setting, a resonance curve was taken with the field in each of the two possible directions in order to average out the effect of the earth's magnetic field. The resonance curves were plotted, and the centers were located graphically.

For the $F=\frac{3}{2}\rightarrow F=\frac{1}{2}$ interval, three frequency settings were used for both the $M=+\frac{1}{2}$ and the $M=-\frac{1}{2}$ transitions. After correction for quadratic effects, the frequency settings are a linear function of the field center values. These two linear functions have exactly opposite slopes, and thus may be put into a single linear graph if the field values for just one function are

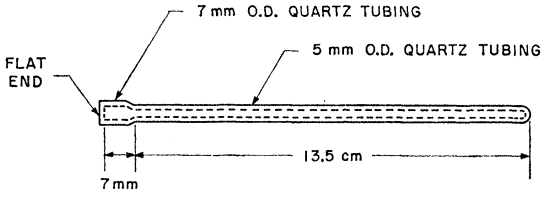

FIG. 8. Resonance cell for 14-kMc/sec transition.

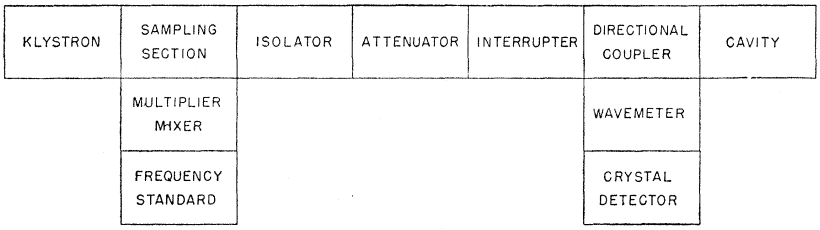

FIG. 9. Schematic diagram of microwave equipment.

taken as negative. The zero-field frequency is then located by the method of least squares.[8]

For the $F=\frac{3}{2}\rightarrow F=\frac{5}{2}$ interval, a similar procedure was used with the $M=\pm\frac{3}{2}$ resonances.

The zero-field frequencies are

$$f(\tfrac{1}{2}\leftrightarrow\tfrac{3}{2})=7551.613\pm0.013 \text{ Mc/sec},$$
$$f(\tfrac{3}{2}\leftrightarrow\tfrac{5}{2})=13\,986.557\pm0.008 \text{ Mc/sec}.$$

The mean lifetime, τ, was approximately 10^{-7} second.

IV. CALCULATIONS FROM THE DATA

The linear part of the hfs may be expressed[9] in frequency units as

$$\tfrac{1}{2}aC+b\left[\frac{\frac{3}{4}C(C+1)-I(I+1)J(J+1)}{2I(2I-1)J(2J-1)}\right],$$

where a is the magnetic dipole interaction constant, by definition; b is the electric quadrupole interaction constant, by definition; and $C=F(F+1)-I(I+1)-J(J+1)$.

The estimated quadratic hfs effect[10,11] is approximately 10^{-4} of the total hyperfine structure. Without explicit calculations of the quadratic effects, the values of the constants are

$$a=-5454.569\pm0.003 \text{ Mc/sec},$$
$$b=-280.107\pm0.005 \text{ Mc/sec}.$$

Calculation of the nuclear dipole moment from a is unnecessary because this moment has been measured directly.[12] Calculation of the quadrupole moment is limited by inaccurate knowledge of wave functions and therefore it was not attempted in this research. The a and b constants can provide information on anomalies,[5,9] dipole moments, and relative quadrupole moments among the mercury isotopes as their $^3P_1$ states are measured.[13]

V. GENERAL REMARK ON THE METHOD

The experimental method discussed in connection with Hg^{201} may be applied, in principle, to any resonant state whose structure, whatever its cause, is larger than its Doppler width.

In the Hg^{201} experiment a natural coincidence of isotopes was employed. When no natural coincidence with an isotope to be measured exists, artificial coincidence can be produced by Zeeman effect or magnetic scanning[14] of the lamp and absorption cell, each of which contains a convenient isotope.

The new double-resonance method described here should be compared with the pioneering polarization-detection experiments.[3,15] Such experiments are not subject to the limitation that the hfs of the excited state be larger than its Doppler width. The new method usually gives higher light fluxes than the old method, particularly if no magnetic scanning is required to produce a coincidence, because large solid angles may be subtended at the scatterer by both the source and the detector and all polarization components of the incident and scattered radiation can be used, lossy polarizers are absent, and the resonance cell may operate at high optical densities.

The signal strength of the new method may be orders of magnitude higher than that of the old, which is usually less than $0.1\bar{P}$ for hfs measurements. In the new method, ϕ may be made arbitrarily small until secondary effects appear. The wings of the absorbing line or isotope impurities in the absorption cell may cause attenuation of the wrong hfs components. The incident light may contain radiation that is not affected by the absorption cell; this radiation might result from isotope impurities in the lamp or from other spectral lines. There may be small spontaneous transfer in the resonance cell from one hyperfine level to another. For such atoms, the resulting reradiation is not affected by the absorption cell.

Higher light fluxes and higher signal strengths result in signal-to-noise ratios that are orders of magnitude higher than those obtainable by the old method. A polarization detection experiment[16] in which the hfs of Hg^{201}, $^3P_1$ was measured in high fields gave a signal-to-noise ratio of less than 5 for saturated

[8] H. Morgenau and G. M. Murphy, *The Mathematics of Physics and Chemistry* (D. Van Nostrand Company, Inc., New York, 1943).

[9] H. Kopfermann, *Nuclear Moments* (Academic Press, Inc., New York, 1958).

[10] C. Schwartz, Phys. Rev. **97**, 380 (1955).

[11] H. Casimir, *On the Interaction between Atomic Nuclei and Electrons* (Teylors Tweede Genootschap, Haarlam, 1936), Vol. 11, p. 36.

[12] B. Cagnac and J. Brossel, Compt. rend. **249**, 77 (1959).

[13] The method described in this paper has now been used by C. V. Stager to measure the hyperfine structure of Hg^{199} and Hg^{197}. An anomaly has been calculated from the hyperfine structure of Hg^{201} and Hg^{199}. [See C. Stager and R. Kohler, Bull. Am. Phys. Soc. **5**, 274 (1960).] Also, C. Brot has measured one frequency interval in Hg^{197*} with this method.

[14] F. Bitter, S. P. Davis, B. Richter, and J. E. R. Young, Phys. Rev. **96**, 1531 (1954).

[15] P. Sagalyn, Phys. Rev. **94**, 885 (1954).

[16] P. Sagalyn, A. Melissionos, and F. Bitter, Phys. Rev. **109**, 375 (1958).

transitions. Measurements of this same hyperfine structure in zero field by the new method, with saturated transitions, have given a signal-to-noise ratio of approximately 5000.

ACKNOWLEDGMENTS

The author is grateful for the support and guidance of Professor Francis Bitter, of Massachusetts Institute of Technology, under whose supervision this research was performed. He wishes to thank Mr. E. Bardho for his invaluable services in building a great deal of the equipment, and Dr. H. H. Stroke and Professor L. C. Bradley, III, for their generous contributions to this work.

APPENDIX. HEAVY ABSORPTION OF SPECTRAL LINE

We shall give expressions for the transmission of light from a single Doppler-broadened spectral line passing through a gas with a Doppler-broadened absorption resonance in the limit of small transmission.[17,18]

The relative transmission, ϕ, can be expressed as an integral[19]:

$$\phi(\mu,\beta,y) = \left(\frac{\beta}{\pi}\right)^{\frac{1}{2}} \int_{-\infty}^{-\infty} \exp\{-[\mu \exp(-x^2)+\beta(x+y)^2]\}dx. \quad (1)$$

The following symbols will be used: [1]=the incident line, [2]=the absorbing line, T=absolute temperature, M=gram molecular weight, ν_1=center frequency of line [1], n=density of molecules in the absorbing gas, l=path length of light in the gas, σ_0=cross section for absorption of the center of absorption resonance,

$$x=\left(\frac{\nu-\nu_2}{\nu_2}\right)\left(\frac{M_2c^2}{2RT_2}\right)^{\frac{1}{2}}, \quad y=\left(\frac{\nu_1-\nu_2}{\nu_2}\right)\left(\frac{M_2c^2}{2RT_2}\right)^{\frac{1}{2}},$$

$$\beta=\frac{T_2}{T_1}\frac{M_1}{M_2}\frac{\nu_2}{\nu_1}, \quad \mu=\sigma_0 nl.$$

For the special case $y=0$,

$$\phi(\mu,\beta)\approx\frac{\Gamma(\beta)}{\mu^\beta}\left(\frac{\beta}{\pi \ln(\mu/\beta)}\right)^{\frac{1}{2}}, \quad \text{for} \quad \mu^\beta/\beta \gg e.$$

For the general case, $\phi=\phi_1+\phi_2$,

$$\phi_1(\mu,\beta,y)\approx\left(\frac{\beta}{\pi}\right)^{\frac{1}{2}}\frac{\exp[-\beta(a_1-y)^2]\Gamma(\rho_1)}{2a_1(\rho_1{}^{\rho_1})},$$

$$\phi_2(\mu,\beta,y)\approx\left(\frac{\beta}{\pi}\right)^{\frac{1}{2}}\frac{\exp[-\beta(a_2+y)^2]\Gamma(\rho_2)}{2a_2(\rho_2{}^{\rho_2})},$$

in which

$$a_1=+\left(\ln\frac{\mu a_1}{\beta(a_1-y)}\right)^{\frac{1}{2}}, \quad a_2=+\left(\ln\frac{\mu a_2}{\beta(a_2+y)}\right)^{\frac{1}{2}},$$

$$\rho_1=\beta(a_1-y)/a_1, \quad \rho_2=\beta(a_2+y)/a_2.$$

The equations for ϕ_1 and ϕ_2 are valid if

$$|\beta y/4\rho_1{}^2a_1{}^3| \ll 1, \quad |\beta y/4\rho_2{}^2a_2{}^3| \ll 1,$$
$$|\rho_1 a_1{}^2| \gg 1, \quad |\rho_2 a_2{}^2| \gg 1,$$
$$\exp(a_1{}^2) \gg 1, \quad \exp(a_2{}^2) \gg 1.$$

It must be noted that the theory in this Appendix assumes Gaussian lines and no coherence among scattering molecules in the gas. However, real optical spectral lines are Gaussian with Lorentzian tails,[20] and real gases display some coherence in scattering.[21]

[17] R. H. Kohler, Quarterly Progress Report No. 52, Research Laboratory of Electronics, Massachusetts Institute of Technology, January 15, 1959 (unpublished), pp. 32–37.

[18] R. H. Kohler, Ph.D. thesis, Department of Physics, Massachusetts Institute of Technology, August, 1960 (unpublished).

[19] J. E. R. Young, Ph.D. thesis, Department of Physics, Massachusetts Institute of Technology, July, 1956, (unpublished).

[20] A. Mitchell and M. Zemansky, *Resonance Radiation and Excited Atoms* (Cambridge University Press, New York, 1939).

[21] R. Dicke, Phys. Rev. **93**, 99 (1954).